Journal of
# Materials Chemistry C

# Absence of delayed fluorescence and triplet-triplet annihilation in organic light emitting diodes with spatially orthogonal bianthracenes

# Absence of delayed fluorescence and triplet-triplet annihilation in organic light emitting diodes with spatially orthogonal bianthracenes

Yong-Jin Pu*[1,2], Rei Satake[2], Yuki Koyama[1,2], Takahiro Otomo[2], Rika Hayashi[3], Naoki Haruta[4], Hiroshi Katagiri[2], Daisuke Otsuki[2], DaeGwi Kim[5], Tohru Sato[4,6,7]

[1]RIKEN Center for Emergent Matter Science (CEMS), Wako, Saitama 351-0198, Japan.

[2]Graduate School of Organic Materials Science, Yamagata University, Yonezawa, Yamagata 992-8510, Japan.

[3]Undergraduate School of Industrial Chemistry, Faculty of Engineering, Kyoto University, Nishikyo-ku, Kyoto 615-8510, Japan

[4]Department of Molecular Engineering, Graduate School of Engineering, Kyoto University, Nishikyo-ku, Kyoto 615-8510, Japan.

[5]Department of Applied Physics, Osaka City University, Osaka 558-8585, Japan.

[6]Fukui Institute for Fundamental Chemistry, Kyoto University, Takano Nishihiraki-cho 34-4, Sakyo-ku, 606-8103 Kyoto, Japan.

[7]Unit of Elements Strategy Initiative for Catalysts & Batteries, Kyoto University, Nishikyo-ku, Kyoto 615-8510, Japan.

*Email - yongjin.pu@riken.jp

## Abstract

Two compounds, 2-methyl-9,10-bis(naphthalen-2-yl)anthracene (MADN), which has a single anthracene unit, and 10,10'-diphenyl-9,9'-bianthracene (PPBA), which has two spatially orthogonal anthracene units, were compared and investigated in terms of photoelectric characteristics and the reverse intersystem crossing (RISC) process in organic light emitting diodes (OLEDs). Transient electroluminescence (EL) measurements indicated large contributions of triplet-triplet annihilation (TTA) for MADN but almost no contribution of TTA for PPBA. Magnetic field dependence of EL for the two anthracene compounds were also different. EL of MADN was sensitive to the magnetic field at high current density, but PPBA showed less dependence, which indicated the absence of the TTA process for PPBA. TD-DFT calculation revealed that PPBA has doubly degenerate lowest triplet states ($T_1$ and $T_2$) with much lower energy than $S_1$, which is unfavorable to thermally activated delayed fluorescence (TADF). Near-zero $\Delta E_{ST}$ between highly excited states $S_{m \geq 1}$ and $T_{n > 2}$ is favorable to RISC at a highly excited state. Oxygen quenching of photoluminescence only for PPBA and decreasing EL intensity with decreasing temperature only for PPBA support the existence of the RISC path from $T_{n > 2}$ to $S_{m \geq 1}$. A high external quantum efficiency of 11% in the blue OLEDs with

PPBA was obtained, indicating that this orthogonal anthracene type molecular design for the RISC at a highly excited state would expand material development of compounds emitting blue fluorescence for OLEDs.

## Introduction

Organic light emitting diodes (OLEDs) have thus far been used as an efficient lighting source in applications such as general lighting, electric signage, and displays for smartphones and televisions. OLEDs have several advantages over other inorganic lighting sources in terms of solution processability and flexibility. On the other hand, improvement of energy conversion efficiency from electricity to light must be developed for lighting sources to save energy consumption.

Phosphorescent complexes that have rare heavy metals such as iridium or platinum can achieve 100% of internal quantum efficiency (IQE) by utilizing triplet excitons that are generally non-radiative in fluorescent molecules resulting in much less efficiency than that of the phosphorescent devices. However, fluorescent compounds for OLEDs are preferred over phosphorescent compounds because the practical long lifetimes of phosphorescent devices, especially blue-emitting devices, are more difficult to achieve.[1] Thus, improving the efficiency of fluorescent OLEDs to the level of phosphorescent OLEDs remains a challenge.

Two approaches to convert non-emissive triplet excitons to emissive singlet excitons in fluorescent molecules have been put forward: triplet-triplet annihilation (TTA)[2,3] and thermally activated delayed fluorescence (TADF)[4-7]. TTA is the triplet up-conversion process from two low-energy triplet excitons ($2 \cdot T_1$) to one high-energy singlet exciton ($S_1$); here, IQE is expected to increase from 25% to 62.5%. Delayed electroluminescence (EL) derived from the spin conversion process is a noticeable characteristic of the TTA process. On the other hand, TADF is the reverse intersystem crossing (RISC) process from one triplet exciton ($T_1$) to one singlet exciton ($S_1$), and thus 100% of IQE can be achieved. This process is conducted by reducing the energy gap between $S_1$ and $T_1$ states ($\Delta E_{ST}$), which is generally large due to the electron exchange energy between these two states. TADF is also characterized by delayed fluorescence and delayed EL.

In addition to the TTA and TADF approaches, the RISC at a higher energy state, intermolecular electron-hole pair state (i.e. hot charge transfer (CT) state)[8,9] or higher excited state ($T_{n \geq 2}$) via the relaxation process[10-12] has been proposed. It is hard to control $\Delta E_{ST}$ or make it near-zero at the intermolecular electron-hole pair state because $\Delta E_{ST}$ is heavily dependent on the molecular packing of its two neighboring molecules, whose spatial positions are almost random in the amorphous state. On the other hand, in a single molecule, making $\Delta E_{ST}$ near-zero at higher excited states is not dependent on the morphology. Suppressing relaxation from $T_n$ to $T_1$ is also important in promoting the RISC path from $T_n$ to $S_{m > 1}$, and relaxation from $S_m$ to $S_1$ has to be allowed if the energy level of

$T_n$ is close to that of $S_{m>1}$ rather than $S_1$. Sato *et al.* theoretically demonstrated that in fluorescent aromatic molecules, symmetry of frontier orbitals influences the selection rules for the electric dipole transition, intersystem crossing, and nonradiative vibronic (electron-vibration) transitions.[11, 13] Furthermore, Sato *et al.* have proposed, as a novel emitting mechanism, the *fluorescent via higher triplet* (FvHT) mechanism, in which a pseudo degenerate excited electronic structure plays a crucial role in suppressing relaxation from $T_n$ to the lower triplet states.[13]

In this study, we compared 2-methyl-9,10-bis(naphthalen-2-yl)anthracene (MADN), a compound having a single anthracene unit, and 10,10'-diphenyl-9,9'-bianthracene (PPBA), a compound having two spatially orthogonal anthracene units, in terms of photoelectric characteristics and the RISC process in OLED devices. Chemical structures of the compounds are shown in Fig. 1a. The OLEDs with PPBA having two spatially orthogonal anthracenes as a non-doped emitter showed an absence of delayed electroluminescence, while the OLEDs with MADN having a single anthracene unit exhibited a large delayed electroluminescence component derived from reproduced singlet excitons through the TTA process. Magnetic field dependence of the devices with MADN was negative due to suppression of the TTA process, whereas the devices with PPBA showed small positive dependence on the magnetic field, also supporting the absence of the TTA process. TD-DFT calculation revealed that isolated PPBA has doubly degenerate lowest triplet states ($T_1$ and $T_2$) with much lower energy than $S_1$ in the Franck-Condon state, and near-zero $\Delta E_{ST}$ between highly excited states $S_{m \geq 1}$ and $T_{n > 2}$. Small vibronic coupling constants between $T_n$ and $T_{1,2}$ support the forbidden transition from $T_n$ to $T_{1,2}$. Oxygen quenching of PL only for PPBA, and decreasing EL intensity with decreasing temperature only for PPBA, support the existence of the RISC path from $T_{n > 2}$ to $S_{m \geq 1}$, which is neither the TTA nor TADF processes involving the $T_{1,2}$ state. This is consistent with calculations of TD-DFT, which suggest a FvHT mechanism with negative $\Delta E_{ST}$ between $T_5$ and $S_3$.

**Results and discussion**

The molecular structure of PPBA was determined by single-crystal X-ray analysis (Fig. 1b). The two covalently linked anthracene groups at the 9,9'-positions are spatially orthogonal to each other. UV-vis spectra of the compounds are shown in Fig. S1. PPBA shows three absorption peaks derived from vibronic structures at the same position as the peaks of MADN, suggesting that the $S_0$-$S_1$ transition of PPBA is based on a localized single anthracene unit. On the other hand, the two compounds showed different PL spectra in solution (Fig. 1c). As reported in a previous study on 9,9-bianthryl[14-16], PPBA comprising a 9,9-bianthryl structure showed red-shifted PL spectra in polar solvents, demonstrating the formation of intramolecular CT excited state in the solution, while PL of MADN was not dependent on the polarity of the solvent, but rather ascribed to localized emission from the anthracene unit.

The PL lifetime of the neat films and the 1wt%-doped films $N,N'$-dicarbazolyl-4,4'-biphenyl (CBP) was measured (Fig. S2 and Table S1). Both the compounds showed only nano second order prompt decay without the micro second order delayed component characterized as the emission of TADF compounds. The PL of the MADN-doped films showed single exponential transience with a lifetime of 4.4 ns. On the other hand, PPBA showed double exponential decay and consisted of the components with a lifetime of 3.5 ns and another component with a lifetime of 9.6 ns, supporting the notion that emission of PPBA in CBP partially includes CT-like features. The transient PL of the neat films was close to instrument response function, and the lifetime was around 1 ns.

Non-doped OLEDs with a ITO/1,1'-bis(di-4-tolyl-aminophenyl)cyclohexane (TAPC) (40 nm)/MADN or PPBA (20 nm)/ 1,3-bis[3,5-di(pyridin-3-yl)phenyl]benzene (B3PyPB) (40 nm)/LiF (1 nm)/Al (80 nm) structure and doped OLEDs with a ITO/TAPC(40 nm)/CBP: 1wt% MADN or PPBA (20 nm)/B3PyPB(40 nm)/LiF(1 nm)/Al(80 nm) structure were fabricated. Current density–voltage and luminance–voltage plots are shown in Fig. S3, and the efficiencies are summarized in Table S2. Delayed EL was measured just after applying a forward-pulse voltage and under applying $-2$ V of the reverse-pulse voltage to eliminate any trapped charges (Fig. 2). The devices with 1wt%-doped emitting layer of MADN and PPBA showed less delayed EL indicating that the contribution of the TTA process is small due to diluted triplet excitons in the doped film. TTA is a bimolecular process that converts two triplet excited states to one singlet exited state and one singlet ground state; thus, the intensity of delayed EL is considered proportional to the square of the current density. In the device with non-doped MADN, the intensity of the delayed EL component clearly increased as current density increased, indicating a large TTA process contribution. In contrast to MADN, the device with non-doped PPBA showed a shorter delay of the EL component and almost no dependence on current density. This result demonstrated the absence of the TTA process in the non-doped PPBA device. There are two likely reasons for this; the first is that $T_1$ excitons with 1.7-1.8 eV on the anthracene unit are not produced through the electrical excitation and relaxation process. Another one is the existence of a faster quenching process of $T_1$ excitons compared to the TTA process, possibly caused by low $T_1$ impurity. However, the latter is less likely because the compounds were thoroughly purified by silica gel column chromatography and train sublimation, after which no impurities were detected by HPLC.

With MADN, external quantum efficiency (EQE) of the non-doped emitting layer (EML) device was higher than that of the doped EML device, although the photoluminescent quantum yields (PLQY) of the MADN neat film are lower than that of doped MADN in CBP (Fig. 3). This result also supports the large contribution of the TTA process in the non-doped MADN device. Contrary to MADN, the non-doped EML device with PPBA showed lower efficiency than that of the doped device. This is attributable to lower PLQY of the PPBA neat film compared to that of doped PPBA

in CBP and supports almost no contribution of the TTA process of PPBA. In the doped devices, PPBA showed much higher EQE than MADN. Maximum EQE for PPBA was 11%, which is one of the highest values ever reported for blue fluorescence OLEDs. The EQE decreased as current density decreased. This negative current dependence also does not support the TTA process and suggests the existence of another RISC path. We also consider that the large roll-off of the efficiency should stems from dissociation of the excitons under high electric filed, because the higher excited states involved in the blue emission are close to energy level of hot carriers. Suppression of the efficiency roll-off is challenging and currently studied. Previously Hu et al reported the similar bianthracene compounds showing highly efficient blue EL.[17] Those compounds also showed less dependence of transient EL on current density and large roll-off of EQE. Hu et al mentioned that high EQE was caused by efficient TTA process, but now we suppose that the previously reported bianthracene compounds also involved the same mechanism in this study.

Magnetic field dependence of EL, shown in Fig. 4, was measured to further investigate the contribution of the TTA process, which is known to exhibit negative dependence on the magnetic field due to Zeeman splitting of the $T_1$ state.[3, 18, 19] The device structure is the following: ITO/conductive polyamine (30 nm)/NPD(35 nm)/ MADN or PPBA (20 nm)/TPBi(40 nm)/LiF(1 nm)/Al. The hole injection layer, hole transporting layer, and electron transporting layer were changed to more stable materials compared to those of the device in the transient EL measurement in order to reduce degradation of the devices because the magnetic field dependence measurement requires a longer time. The device with non-doped MADN showed positive dependence on the magnetic field in low current density due to suppression of hyper fine coupling; however, as current density increased, the magnetic field dependence become negative due to suppression of the TTA process, which increases EL intensity. Contrary to MADN, the device with non-doped PPBA showed only small positive dependence on the magnetic field.

Quantum chemical calculations at the TD-DFT B3LYP/6-311+G(d,p) level of theory revealed that PPBA has pseudo degenerate lowest triplet states ($T_1$ and $T_2$) that are lower in energy than $S_1$ at the Franck-Condon state by 1.11 eV (Fig. 5). The singlet-triplet energy gap is too large for TADF. The excitation energy of the lowest triplets is 1.75 eV, and that of the lowest singlet state is 2.85 eV. These results suggest that the emitting mechanism observed in PPBA is not the TADF mechanism.

The symmetry of the optimized structure is $D_{2d}$, and the irreducible representations (irreps) of $S_1$, $S_2$, and $S_3$ are $A_2$, $B_1$, and $B_3$, respectively. It should be noted that, for an electric dipole transition to $S_0$, $B_3$ irrep is symmetry-allowed, and $A_2$ and $B_1$ are symmetry-forbidden. We performed a geometry optimization for the $B_3$ $S_3$ state and obtained the $B_3$ $S_3$ adiabatic state with an emitting wavelength of 443 nm and an oscillator strength of 0.3181. The calculated wavelength is consistent with the experimental observation. The singlet states lower than the $B_3$ $S_3$ adiabatic state are still symmetry-

forbidden. Therefore, we assign the fluorescent state to the $B_3$ $S_3$ state. This indicates that the radiative/non-radiative transitions from $S_3$ to the lower singlet states should be suppressed. Such anti-Kasha's rule behavior can be explained by the multiconfigurational structure of the electronic wavefunction as discussed in Ref. 12. We calculated the energy levels with optimization at each higher triplet state, and found that the optimized $T_5$ state is slightly lower than the $S_3$ state with near-zero $\Delta E_{ST}$ = -21 meV. Small offdiagonal vibronic coupling constants are expected between $T_5$ and the lower triplet states, which suggest the suppressed transition from $T_5$ because of the multiconfigurational structure of the electronic wavefunction of $T_5$.[13]

   PL quenching by oxygen, shown in Fig. 6, showed a clear difference between MADN and PPBA. PL spectra in toluene solution after argon bubbling or oxygen bubbling for 20 min in a 10 ml volumetric flask were measured. The PL intensity of MADN was almost not quenched by oxygen, although PPBA exhibited large quenching by oxygen. This result suggests that the exciton at $S_1$ state on the monoanthracene MADN cannot be transferred to the $T_1$ state via intersystem crossing, but the exciton at the $S_1$ state on the orthogonal bianthracene PPBA can be transferred to $T_1$ and finally quenched by triplet oxygen. However, the $S_1$ exciton at the local monoanthracene cannot be directly transferred to the $T_1$ state as indicated by MADN. Therefore, in PPBA, the $S_1$ exciton should be transferred to the $T_{1,2}$ state through the $T_{n>2}$ state.

   Temperature dependence of EL intensity can provide us with useful information on the energy difference between the triplet state and the excited singlet state (Fig. 7). If reverse intersystem crossing from the triplet state to the excited singlet state occurs endothermically, EL intensity should decrease as temperature decreases. However, in non-doped devices, EL intensity of both MADN and PPBA increased as temperature decreased. This is because PL intensity largely increased as temperature decreased due to suppression of nonradiative quenching by vibrational relaxation (Fig. S4). On the other hand, EL intensity of the doped device for PPBA decreased as temperature decreased, while the doped device for MADN showed almost the same EL intensity to temperature. The negative dependence of PPBA on decreasing temperature cannot be attributed to changes in the PLQY because the CBP host of the doped film of MADN and PPBA suppressed the concentration quenching and the PL intensity was less sensitive to temperature. In the doped films, the contribution of TTA to RISC is small, shown by the absence of delayed EL (Fig. 2). Therefore, these results indicate that PPBA has an RISC path other than the $T_{1,2}$ state to the excited singlet state.

**Conclusions**

Monoanthracene compound MADN and spatially orthogonal bianthracene compound PPBA showed different photophysical and electroluminescent properties. Transient EL measurement and magnetic field dependence of EL revealed large TTA contributions of MADN and no contribution of PPBA.

PL quenching by oxygen and negative temperature dependence of EL only for PPBA support the FvHT mechanism with RISC from $T_{n > 2}$ to $S_{m \geq 1}$, suggested by the TD-DFT calculation. High EQE of 11% for PPBA in blue OLEDs demonstrate the practical effectiveness of the molecular design.

## Conflicts of interest

There are no confricts to declare.

## Acknowledgement

## Notes and references

1. J. Lee, C. Jeong, T. Batagoda, C. Coburn, M. E. Thompson and S. R. Forrest, *Nat. Commun.*, 2017, **8**, 15566.
2. D. Y. Kondakov, *J. Appl. Phys.*, 2007, **102**, 114504.
3. D. Y. Kondakov, T. D. Pawlik, T. K. Hatwar and J. P. Spindler, *J. Appl. Phys.*, 2009, **106**, 124510.
4. H. Uoyama, K. Goushi, K. Shizu, H. Nomura and C. Adachi, *Nature*, 2012, **492**, 234-238.
5. A. Endo, M. Ogasawara, A. Takahashi, D. Yokoyama, Y. Kato and C. Adachi, *Adv. Mater.*, 2009, **21**, 4802-4806.
6. Y. Tao, K. Yuan, T. Chen, P. Xu, H. H. Li, R. F. Chen, C. Zheng, L. Zhang and W. Huang, *Adv. Mater.*, 2014, **26**, 7931-7958.
7. T. T. Bui, F. Goubard, M. Ibrahim-Ouali, D. Gigmes and F. Dumur, *Beilstein J. Org. Chem.*, 2018, **14**, 282-308.
8. S. Difley, D. Beljonne and T. Van Voorhis, *J. Am. Chem. Soc.*, 2008, **130**, 3420-3427.
9. M. Segal, M. Singh, K. Rivoire, S. Difley, T. Van Voorhis and M. A. Baldo, *Nat. Mater.*, 2007, **6**, 374-378.
10. L. Yao, S. T. Zhang, R. Wang, W. J. Li, F. Z. Shen, B. Yang and Y. G. Ma, *Angew. Chem. Int. Ed.*, 2014, **53**, 2119-2123.
11. T. Sato, M. Uejima, K. Tanaka, H. Kaji and C. Adachi, *J. Mater. Chem. C*, 2015, **3**, 870-878.
12. W. J. Li, Y. Y. Pan, R. Xiao, Q. M. Peng, S. T. Zhang, D. G. Ma, F. Li, F. Z. Shen, Y. H. Wang, B. Yang and Y. G. Ma, *Adv. Funct. Mater.*, 2014, **24**, 1609-1614.
13. T. Sato, R. Hayashi, N. Haruta and Y.-J. Pu, *Sci. Rep.*, 2017, **7**, 4820.
14. K. Hara, T. Arase and J. Osugi, *J. Am. Chem. Soc.*, 1984, **106**, 1968-1972.
15. T. J. Kang, M. A. Kahlow, D. Giser, S. Swallen, V. Nagarajan, W. Jarzeba and P. F. Barbara, *J. Phys. Chem.*, 1988, **92**, 6800-6807.
16. Y. Yu, L. Ma, X. L. Yang, H. X. Zhou, H. L. Qin, J. L. Q. Song, G. J. Zhou, D. D. Wang and Z. X. Wu, *Adv. Opt. Mater.*, 2018, **6**, 1800060.
17. J.-Y. Hu, Y.-J. Pu, F. Satoh, S. Kawata, H. Katagiri, H. Sasabe and J. Kido, *Adv. Funct. Mater.*, 2014, **24**, 2064-2071.
18. Q. M. Peng, W. J. Li, S. T. Zhang, P. Chen, F. Li and Y. G. Ma, *Adv. Opt. Mater.*, 2013, **1**, 362-

366.

19.  R. C. Johnson and R. E. Merrifield, *Phys. Rev. B*, 1970, **1**, 896-902.
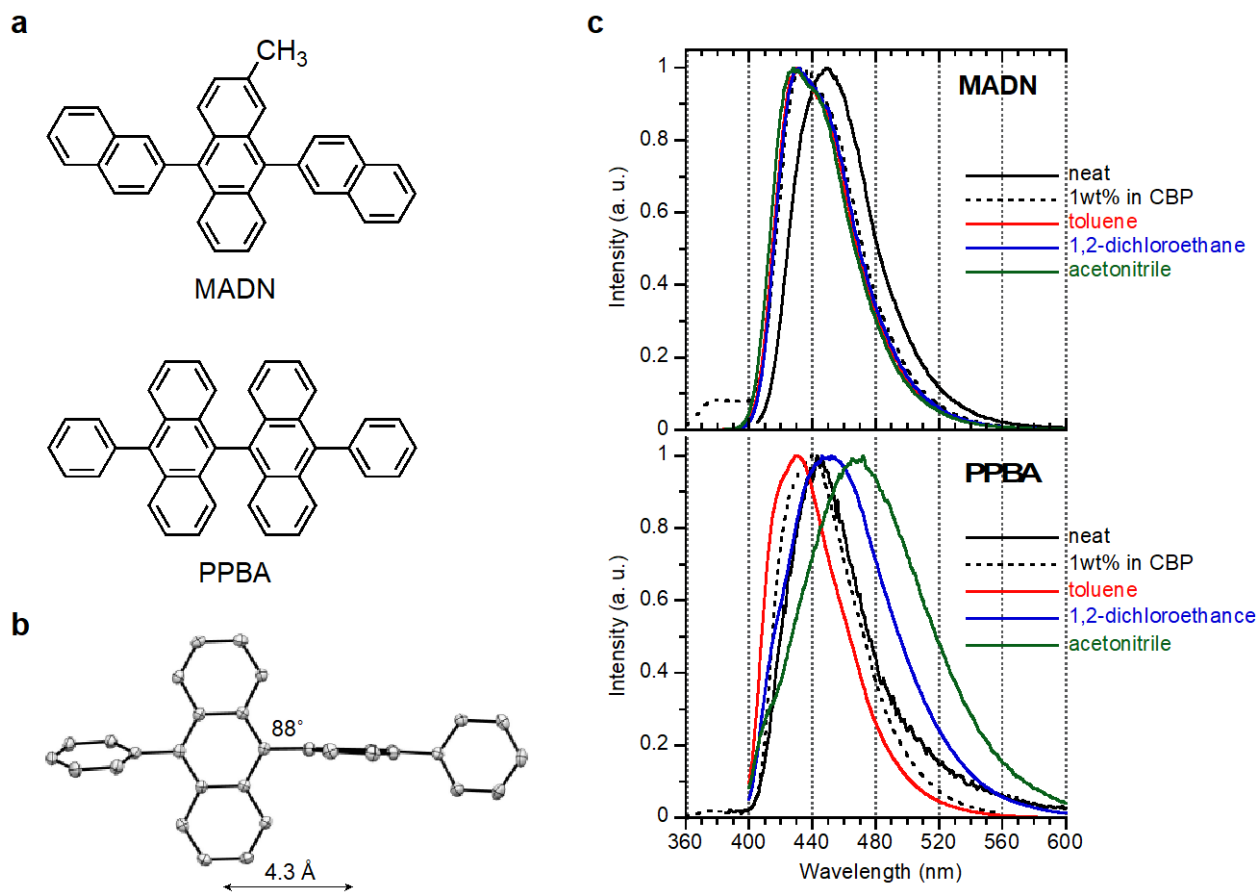
**Fig. 1** (a) Chemical structure of MADN and PPBA. (b) Molecular structure of PPBA obtained by single-crystal X-ray analysis, depicting dihedral angle and distance between centroids of the two anthracenes. (c) PL spectra of MADN and PPBA.
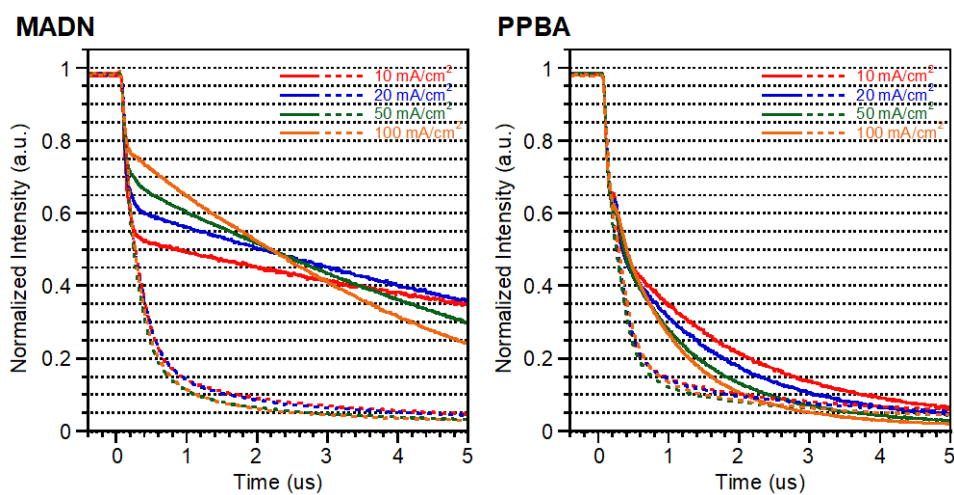


**Fig. 2** Transient EL of the non-doped devices (solid line) and the doped device (dotted line).
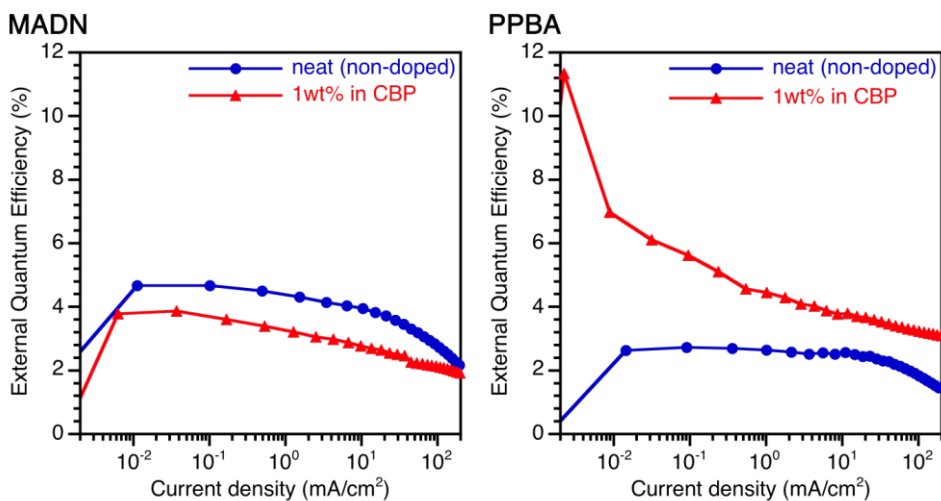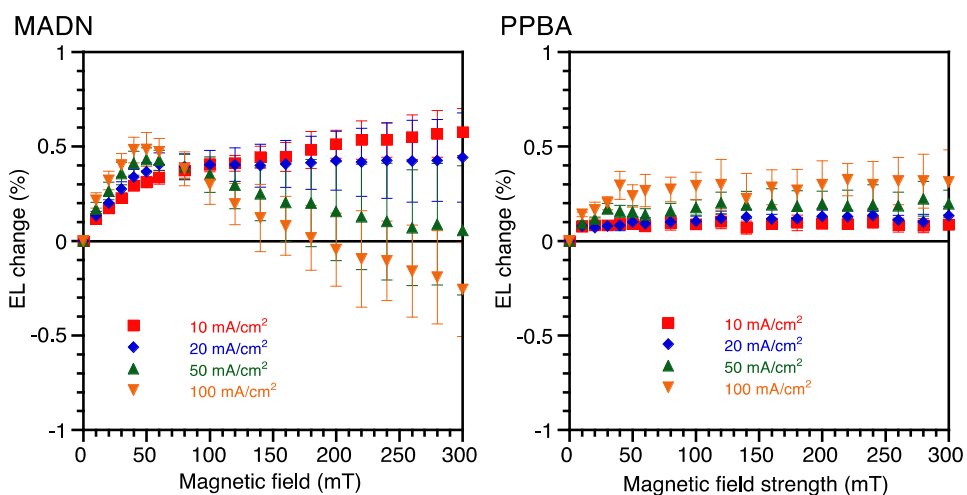
**Fig. 3** EQE–current density plots.
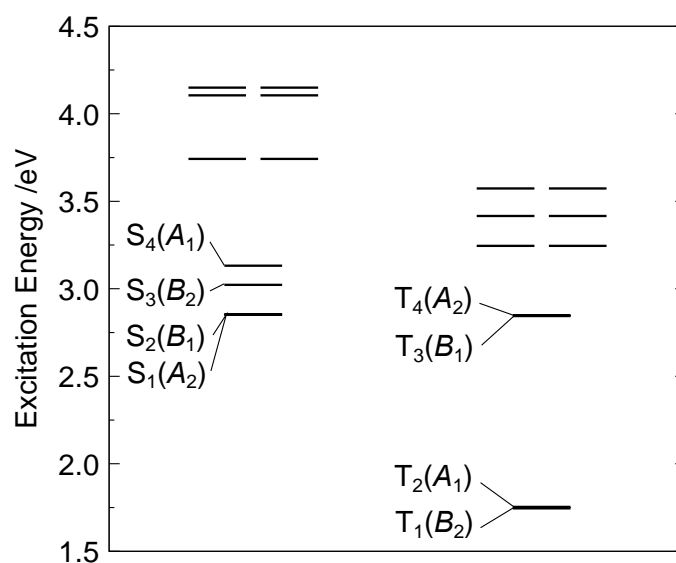


**Fig. 4** Magnetic field dependence of EL.



**Fig. 5** Energy diagram of PPBA in the Franck-Condon state obtained by TD-DFT calculation.
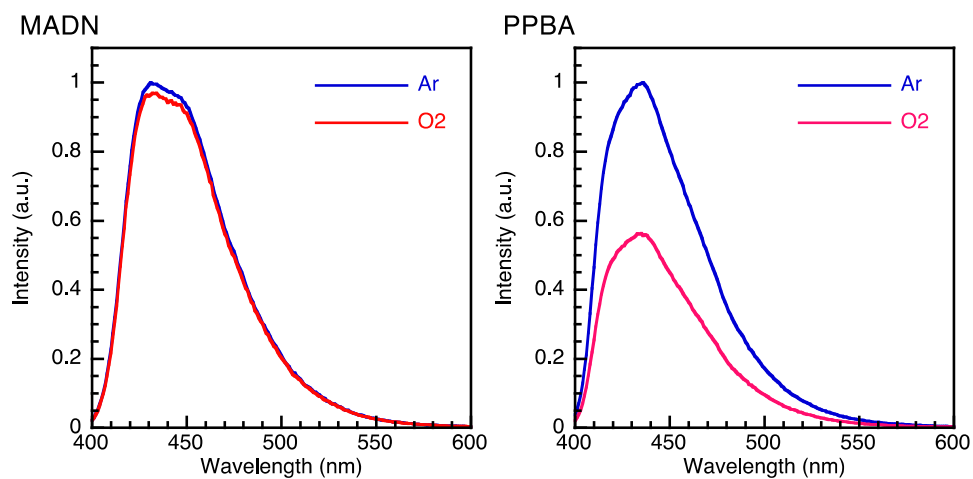
**Fig. 6** PL spectra in toluene solution after argon bubbling and oxygen bubbling
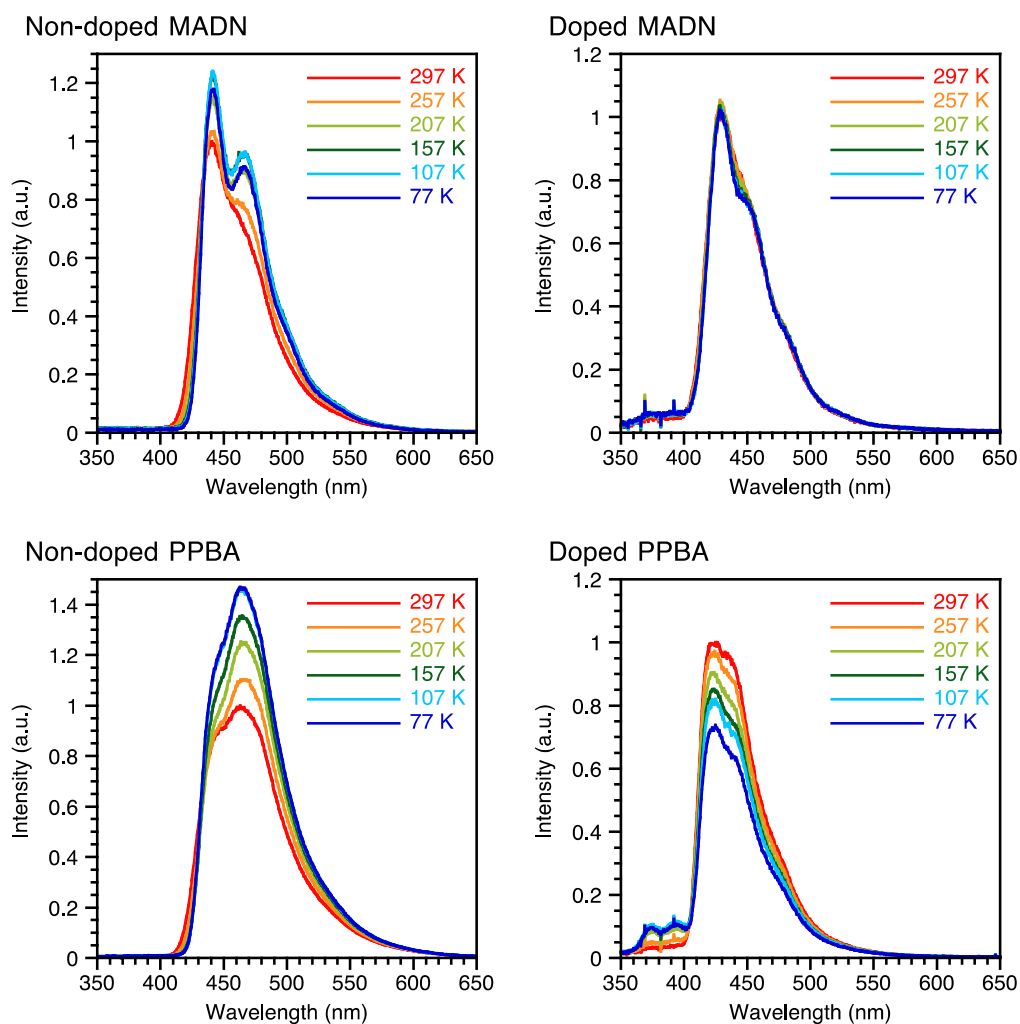


**Fig. 7** Temperature dependence of EL

10,10'-Diphenyl-9,9'-bianthracene (PPBA) does not generate $T_1$ excitons in OLEDs, and RISC at higher excited state is suggested.



**PPBA**